



LAWRENCE
LIVERMORE
NATIONAL
LABORATORY

Characterization of Electron Beams in Multiple Welders Using the Enhanced Modified Faraday Cup

T. A. Palmer, J. W. Elmer

August 7, 2006

International Institute of Welding
Quebec City, Canada
August 27, 2006 through September 2, 2006

Disclaimer

This document was prepared as an account of work sponsored by an agency of the United States Government. Neither the United States Government nor the University of California nor any of their employees, makes any warranty, express or implied, or assumes any legal liability or responsibility for the accuracy, completeness, or usefulness of any information, apparatus, product, or process disclosed, or represents that its use would not infringe privately owned rights. Reference herein to any specific commercial product, process, or service by trade name, trademark, manufacturer, or otherwise, does not necessarily constitute or imply its endorsement, recommendation, or favoring by the United States Government or the University of California. The views and opinions of authors expressed herein do not necessarily state or reflect those of the United States Government or the University of California, and shall not be used for advertising or product endorsement purposes.

Characterization of Electron Beams in Multiple Welders Using the Enhanced Modified Faraday Cup

T.A. Palmer and J.W. Elmer

Lawrence Livermore National Laboratory, Livermore, CA

Abstract

Using the Enhanced Modified Faraday Cup (EMFC), the differences in the beams produced by two electron beam (EB) welders are characterized at different focus settings and work distances. For example, EMFC measurements show that sharply focused beams display different shapes and peak power densities which vary by nearly 20% for the same welding parameters on these two welders. Increases in work distance on each machine were shown to result in decreases in both the peak power density and the resulting weld size and shape. Because of the differences in machine performance, additional differences arise when comparing the welds produced by each machine. These different weld dimensions are attributed to differences in the beam shape and a 70 mm difference in the theoretical beam crossover location in the upper column of the two welders. The crossover location, which can not be physically measured, is determined using the EMFC by analyzing the beam distribution parameters of sharply focused beams over a range of work distances and can be used to explain the variation in the peak power densities of the two machines. Once the machines are characterized using this quantitative tool, changes in either the beam focus or work distance can be made to attain similar beams from different welders, thus providing a baseline for developing modern weld transfer procedures.

Introduction

The power density distribution in electron beams is controlled primarily by choices in the accelerating voltage, beam current, and focus coil current setting. These settings, along with the choice of travel speed, work distance, and vacuum level, are also the primary process parameters used in electron beam (EB) welding to produce a weld of a given size and shape. Almost all of these process parameters are quantifiable and tightly controlled prior to and during the welding process, except for the determination of the “sharp focus” condition of the beam, which is controlled by the focus coil current.

It is difficult to define and reproduce the “sharp focus” condition on a consistent basis because of the manual nature in which beam focusing is performed. During focusing, the strength of the magnetic lens in the focus coils is manually adjusted by the operator, thus arbitrarily raising or lowering the sharp focus position in the weld chamber. In order to determine the sharp focus setting, the operator directs the beam onto a high melting point target material, such as tungsten, and adjusts the focus coil current setting while observing the intensity of the light emitted from the target. When the emitted light reaches a maximum intensity, the beam is considered to be at sharp focus.[1]

The reproducibility of a sharply focused beam at a given focus setting on even a single machine is not guaranteed. Different operators may interpret the brightest emission from the target material differently, resulting in different definitions of “sharp focus.” As a result, beams with different properties may be mistakenly used in the welding of potentially high-value components. These difficulties are only compounded when the parameters selected for one machine are transferred to other machines. With different machines, the beam produced at a given focus setting on one machine may not match that produced on another, due to differences in the focusing lens and the construction of the upper column of the EB welder. As a result, the current density distribution of each beam can differ, resulting in welds of differing dimensions.

Even though EB welding has been in common usage for several decades, it is only recently that diagnostic tools for providing quantitative information on the properties of electron beams used for welding have become available [2-8]. One such tool is the Enhanced Modified Faraday Cup (EMFC) system, which has been developed and tested at Lawrence Livermore National Laboratory (LLNL).[5-8] This system collects the beam through a series of radial slits as it is oscillated in the shape of a circle over a tungsten disk. Once the data from the beam are

collected, computer tomography algorithms are used to reconstruct the power density distribution of the beam. Based on this reconstruction, several important beam parameters, including measures of the peak power density and beam width, are determined.

Using this diagnostic tool, the effects of changes in the focus setting at constant voltage, current, and work distance on the resulting electron beam parameters have been characterized on two machines, built approximately ten years apart, in use at LLNL. Based on these results, a quantitative definition of the machine sharp focus condition has been made. The responses of the different welders to changes in focus setting are compared, and the relationship between well characterized sharply focused beams and the resulting weld dimensions is determined for each welder.

The results show that these two welders produce beams with different properties at the same machine settings. By monitoring the effects of changes in work distance on the properties of sharply focused beams in each welder, an estimate of the beam crossover location in the upper column of each machine is made. The crossover location can be used to take into account the performance characteristics of each welder and can be used to explain the effects of differences in the upper column on machine performance. Knowledge of this beam parameter can then be used to provide a more definitive definition of the differences in the performance of different welders. Further work will be focused on further refining the correlation between this parameter and the transfer of beam parameters between different welders.

Experimental

Electron Beam Diagnostics

A photograph of the EMFC device and a schematic illustration of its basic components are shown in Figures 1(a) and 1(b), respectively. The current version of this diagnostic tool contains a number of enhancements to previous designs, meant to improve both the performance of the device as well as to improve the quality of the captured data.[9] During use, the EMFC device captures the electron beam as it is deflected along a circular path approximately 25.4 mm in diameter. Unlike a traditional Faraday Cup, which contains a single small hole, the EMFC device contains 17 linear slits placed at radial angles around a tungsten slit disk.

When the beam passes over each slit, a portion of the beam current passes into the Faraday Cup and is converted into a voltage drop across a known resistor. This voltage drop is captured

by a fast sampling analog-to-digital (A/D) converter. Figure 2(a) illustrates a typical voltage drop measured across one of these slits. Each slit samples the beam at a different angle, providing 17 different profiles of the beam shape. After passing over all 17 radial slits, a waveform containing the 17 resulting peaks is captured by the data acquisition software, as shown in Figure 2(b). If necessary, a digital filtering routine is applied to the data to remove any electronic noise which may appear. The data are then fed into a computer assisted tomographic (CT) imaging algorithm in order to reconstruct the power density distribution of the beam (See Figure 2(c)).[8]

Once reconstructed, the peak power density of the electron beam and two distribution parameters are determined. Figure 2(d) shows one slice taken through the reconstructed beam to illustrate how these parameters are determined. The first distribution parameter is the full width of the beam at one-half its peak power density (FWHM). This parameter represents the width at 50% of the beam peak power density. The second parameter is the full width of the beam measured at $1/e^2$ of its peak power density (FW e^2). This parameter represents the diameter of the beam at 86.5% of the beam peak power density. Since the cross section of the measured beam is not always circular, the area of the beam at these two points is measured, and the diameter of a circle having the same area is used to represent both values. These approximations are good for most beams with generally circular cross sectional shapes, such as the Gaussian-like distributions typically found near the sharp focus setting. Both values can generally be used as a means of defining the beam width. However, for non-circular beam shapes, the orientation of the beam may influence the weld geometry.

Characterization of Electron Beam Welders

In this study, the EMFC diagnostic system was used to determine the effects of changes in beam focus setting and work distance on the resulting electron beam properties of two electron beam welding systems in use at LLNL. The general characteristics of these welders are listed in Table 1. Each welder is capable of an accelerating voltage of 150 kV and a beam current of 50 mA and has been produced by the same manufacturer, though there is a difference of ten years in their ages. The focus response for each welder was characterized by measuring the beam properties at focus settings ranging from approximately 30 mA above to 30 mA below the

operator determined sharp focus setting. The change in peak power density, FWHM, and FWe2 values were tracked with changes in the focus settings.

After characterizing the focus response of each machine, autogenous welds were made on 9.5 mm thick 304L stainless steel samples at a constant power of 1 kW and the respective sharp focus setting on each machine. The weld samples were fabricated from material taken from a single heat with a chemical composition of Fe-18.2 Cr-8.16 Ni-1.71 Mn-0.02 C-0.082 N-0.47 Mo-0.44 Si-0.14 Co-0.35 Cu-0.0004 S-0.03 P. All values are in wt.%. After welding, a single sample was removed from each weld at a location approximately halfway between the beginning and end of the weld and mounted in cross section. Each weld pool cross section was metallographically prepared and etched using an electrolytic oxalic acid solution to expose the fusion zone. Measurements of the depth, width, and melted area were then made on each cross section using Image Pro, Version 4.1.* The results obtained from the different welders were then compared.

In a second set of experiments, the effects of changes in work distance on the focus response of electron beams produced by each of the welders were examined. Work distances range between 127 mm and 508 mm for the two welders. These work distances are based on measurements made from the interior top of the vacuum chamber to the top of the tungsten slit disk on the EMFC. The maximum work distance examined for each welder varies with the size of the vacuum chamber, and the minimum work distance is determined by the ability of the deflection coils to produce a 25.4 mm diameter circle. An autogenous weld was then made on a 304L stainless steel weld sample at the sharp focus setting at each work distance in each welder. This work distance is measured from the top of the vacuum chamber to the top surface of the 304L weld samples, which are placed at the same height as the tungsten slit disk on the EMFC.

Results and Discussion

Measuring the Focus Response of Each Welder

With the EMFC diagnostic tool, the effects of changes in focus settings on the peak power density and the FWHM and FWe2 distribution functions of a 100 kV, 10 mA beam have been analyzed on each welder. A typical example of the relationship between the peak power density and the focus coil current setting is shown in Figure 3(a) for a 100 kV, 10 mA beam produced by

* Image Pro is a trademark of Media Cybernetics, Inc., Silver Spring, MD.

S/N 175 at a work distance of 229 mm. The plot is characterized by a well defined maximum peak power density, which has a value of approximately 20 kW/mm^2 , at a focus setting of 446 mA. With small changes in the focus setting, the corresponding peak power density value rapidly decreases near the sharp focus setting. At the focus settings far removed from this maximum value, though, the measured peak power density values display minimal variation.

The operator determined sharp focus setting (450 mA) is also indicated on the plot for this welder. In the absence of EB diagnostics, this setting would be considered the sharp focus setting and would not be contested. However, the peak power density curve shown in Figure 3(a) displays a maximum value at a focus setting of 446 mA. This difference of 4 mA in focus settings indicates that the operator determined sharp focus setting is not a reliable means for determining the focus setting of the machine at its peak intensity. Therefore, a means for defining the machine sharp focus setting, as opposed to the operator determined sharp focus setting, is required.

With the EMFC diagnostic tool, there are three primary measurements made on each beam, including the peak power density and FWHM and FWe2 beam distribution parameters. In defining the machine sharp focus condition, the effects of changes in the focus settings on each parameter near sharp focus must be well-defined. Of these three parameters, the peak power density appears to be optimal for defining this focus condition, based on its sensitivity to small changes in the focus setting near the maximum peak power density value.

The focus coil current settings required to achieve the sharp focus settings vary between welders due to differences in their electron gun and focus lens designs. It is, therefore, convenient to define a relative setting to describe the same focus condition on different welders. The machine sharp focus setting, as defined above, is used as the reference value and is set to a value of zero for the sharpest focused beams to define the relative machine focus setting. Focus coil current settings above this value are given a positive value, while those below are given a negative value, as shown in the following relationship:

$$\text{Machine Focus Setting} = \text{Focus Coil Current} - \text{Sharp Focus Coil Current} \quad (1)$$

where the focus coil current (mA) is the value for each focus setting and the sharp focus coil current (mA) represents the focus coil current at the machine sharp focus setting. The machine

focus settings represent the amount of defocus above (positive) or below (negative) the sharp focus setting. The focus coil current values plotted in Figure 3(a) have been converted to the corresponding machine focus settings, as shown in Figure 3(b). This convention for defining the machine focus is used exclusively throughout the remainder of this paper when examining the effects of changes in focus on the peak power density, FWHM, and FWe2 values.

A comparison of the reconstructed beams at the machine sharp focus setting of each welder is shown in Figures 4(a) and 4(b) for a 100 kV, 10 mA beam at a work distance of 229 mm. The beams produced by each welder at the respective machine sharp focus settings vary both in shape and power density distribution. S/N 175 displays a slightly oblong shape and has the highest power densities located in the center of the beam. The power densities then decrease rather rapidly as the edges of the beam are approached. On the other hand, S/N 605 produces a fairly round beam at sharp focus with a much more uniform peak power density distribution across the beam diameter and no clearly defined hot spot in the center.

The peak power density, FWHM, and FWe2 values for each welder at its respective machine sharp focus setting are summarized in Table 2 for 100 kV, 10 mA beams and a work distance of 229 mm. Even though the same settings are used on each machine, rather significant variations in the measured beam parameters are observed. For example, S/N 175 displays a peak power density of approximately 20 kW/mm^2 and narrowest beam distribution parameters (FWHM = 0.210 mm and FWe2 = 0.346 mm). S/N 605 displays both a lower peak power density of 15.7 kW/mm^2 and wider beam distribution parameters (FWHM = 0.237 mm and FWe2 = 0.395 mm). Although both beams have the same total power, S/N 605 produces a beam which is 21% lower in peak power density and between 11% and 12% wider, as defined by the FWHM and FWe2 values, respectively, than those observed in the beam produced by S/N 175.

In addition to defining the beam parameters at the machine sharp focus setting, it is equally important to measure the properties of defocused beams. Comparisons of the peak power density, FWHM, and FWe2 values measured over a range of machine focus settings from approximately -30 to +30 on each welder are shown in Figures 5(a-c). Differences in the individual response of each welder to changes in the focus setting are evident. In Figure 5(a), the peak power density values reach a clearly defined maximum value at the machine sharp focus setting for S/N 175. S/N 605 does not display as sharply a defined peak value and shows little change at machine focus settings between +5 and -5.

Both the FWHM and FWe2 values plotted in Figures 5(b) and 5(c) for each welder display minimum values at the machine sharp focus settings and slowly increase in size at higher positive and negative defocus settings. Since these beam distribution parameters increase rather slowly at small defocus settings, the minimum beam width is not as easily discernible as the maximum peak power density. This lack of a clear minimum value for each parameter is the primary reason that the peak power density is used to define the machine sharp focus setting. At high positive and negative defocus settings, the measured beam widths increase markedly, and the differences between the beam widths produced by each welder also increase, especially at positive defocus settings. Much like the situation described in Figure 5(a), S/N 605 does not display as well-defined a minimum at sharp focus as S/N 175 for both beam distribution parameters. These differences in the focus response of the welders illustrate how characteristics of each welder differ, even at the same machine settings.

Based on these results, the utility of the EMFC in characterizing the peak power density, shape, and power density distribution of electron beams is made clear. Even though the welders produce different beams, beams with similar properties can be produced on the two machines by adjusting their respective focus settings. For example, S/N 175 at a machine focus setting of +5 can produce a beam with similar peak power density and FWe2 values as S/N 605 at its machine sharp focus setting. The ability to accurately produce similar beams on different welders is an important consideration in the transfer of beam properties from one machine to another.

Correlation between Beam Diagnostics and Weld Pool Size and Shape

With knowledge of the respective beam characteristics for each welder, the correlation between the beam properties and the resulting weld pool size and shape can be examined. Autogenous welds are first made at the machine sharp focus setting of each welder on a 304L stainless steel sample at an accelerating voltage of 100 kV, a beam current of 10 mA, and a travel speed of 17 mm/sec. Figures 6(a) and 6(b) show the resulting weld cross sections produced by each welder, and Table 2 lists the measurements of the weld width, depth, aspect ratio, and cross sectional area, along with the corresponding sharp focus beam parameters.

Each welder produces similarly shaped weld cross sections, showing keyhole type behavior at the respective machine sharp focus settings. However, differences in the characteristics of sharply focused beams also result in differences in the measured depth and width of each weld.

The measured weld depths produced at the respective machine sharp focus settings show a difference of approximately 7%, with S/N 605 producing the deeper weld. Based on these observations, the higher peak power density weld shows the lower penetration.

The potential for spiking at the weld root can have an effect on the measured weld depth.[10-14] Spiking is typically defined as a sudden increase in penetration above the average line of penetration. It is particularly prevalent when examining the root of the weld in the longitudinal orientation along the direction of welding. Rather than displaying a uniform depth, small protrusions, resulting from instabilities in the weld keyhole, appear at random intervals. When only a single weld cross section is used, it is possible that the transverse cross section may be taken from one of the spikes or accompanying troughs present at the weld root, adding a level of uncertainty to the reported weld depths.

Figure 6(b) provides a pertinent example of this phenomenon in the weld produced by S/N 605. In this case, the depth of the weld at both the top (3.42 mm) and bottom (4.26 mm) of the pore is measured, resulting in a 20% difference in the weld depth. When the depth measurement is made at the top of the pore, the weld produced by S/N 605 is approximately 14% shallower. The measured widths are unaffected by the spiking in the weld root, and S/N 175 produces a weld which is approximately 4% wider than that produced by S/N 605.

Other studies have indicated that beams with higher peak power densities produce deeper welds[15], but the presence of the suspected spiking in the weld produced by S/N 605 complicates such an observation in this case. Only when the depth at the top of the pore is taken into account does this relationship hold true. In this case, S/N 605 produces the shallower weld with a lower peak power density beam. A comparison of the peak power densities of the beams produced by the two machines shows a difference of approximately 22%, while the depths of the two welds differ by 14%. This difference is in line with prior observations of the peak power density weld depth relationship.

The size and shape of the welds produced by each machine can also be affected by the different beam orientations and power density distributions, both of which are not detectable without the use of this diagnostic tool. First, the orientations of the beams vary, as shown in Figure 4(a), with the beam produced by S/N 175 being more elongated along its x axis, which corresponds to the direction of welding. The beam produced by S/N 605, while not entirely circular, lacks the well-defined orientation of that produced by S/N 175. Second, different power

density distributions are measured across the two beam diameters, as shown in Figures 4(a) and 4(b).

Effect of Work Distance on Electron Beam Properties

Changes in work distance can also have a pronounced effect on the properties of sharply focused beams on a given welder. These changes in work distance require a change in the focal length of the electron focusing lens, which is capable of focusing the beam over a range of work distances within the chamber by changing the focus coil current setting. As the focal length of the beam is decreased, the power density of the most sharply focused beam increases along with the divergence angle of the beam exiting the EB optics in the upper column. With the increase in the divergence angle of the beam, which occurs at shorter work distances, small changes in the focus setting near the machine sharp focus condition produce larger changes in the peak power density and beam width than at the longer work distance.

Understanding the effects of different work distances on the beam properties becomes important when comparing the performance of different welders, especially ones having different sized vacuum chambers. These changes in work distance are shown to have a significant impact on the peak power density and beam distribution parameters measured by the EMFC diagnostic tool across a range of focus settings in each welder. Figures 7(a) through 7(c) show the effects of changes in both work distance and focus setting on the peak power density, FWHM, and FWe2 values, respectively, on S/N 175. Similar trends are observed in Figures 8(a) through 8(c) for S/N 605.

At shorter work distances on both welders, the beams display much higher peak power densities and narrower beam distribution parameters at both the machine sharp focus setting and at small defocus settings. The rate of change in the peak power density with changes in focus, especially near the machine sharp focus setting, is also affected by changes in work distance. For example, the peak power density measurements at shorter work distances rapidly decrease with small changes in focus settings above or below the machine sharp focus, resulting in more sharply defined maximum values for the peak power density. With increasing work distance, the slopes of the curves decrease in the vicinity of the machine sharp focus setting and display a more flattened appearance.

The FWHM and FWe2 beam distribution parameters, shown in Figures 7(b) and 7(c), respectively, display generally opposite trends to that observed in the peak power density as a function of work distance. For example, at each work distance, the beams produced at the machine sharp focus setting display the narrowest distribution parameters, then increase as the machine focus setting moves further from sharp focus. With increases in work distance, the beam distribution parameters for the sharply focused beams increase, in contrast to the decrease observed in the peak power density values in Figure 7(a), indicating that the beams are becoming wider. On the other hand, the shapes of the curves for both beam distribution parameters show few differences with changes in work distance.

Summaries of the beam parameters measured at the machine sharp focus settings at work distances between 127 mm and 508 mm in each welder are given in Tables 3 and 4. As shown in these tables, changes in the work distance have a marked effect on the resulting beam parameters of the sharply focused beams, with the shorter work distances displaying significantly higher peak power density values and narrower beam distribution parameters. For example, in S/N 175, an increase of 102 mm in work distance, from 127 mm to 229 mm, results in a decrease of nearly 43% in peak power density and an increase of nearly 25% in the FWHM value. A comparable decrease in peak power density is also observed in S/N 605, as tabulated in Table 4. With this welder, an increase in work distance of 127 mm, from 178 mm to 305 mm, results in a decrease of over 44% in peak power density and an increase of 28% in the FWHM value.

A closer examination of the data indicates that there is a predictable change in the beam distribution parameters measured at the machine sharp focus setting with changes in the work distance. For example, the FWHM and FWe2 values measured at the machine sharp focus settings over a range of work distances in S/N 175 are plotted in Figure 9. Both beam distribution parameters decrease linearly with decreasing work distance. The results of individual linear regression analyses are also shown on the plot, providing relations between the FWHM and FWe2 values and the work distance. Similar relationships are observed between the beam distribution parameters and the work distances on S/N 605.

The FWHM-Work Distance relationships for both welders are plotted in Figure 10(a). The corresponding linear regressions for S/N 175 and S/N 605, respectively, are shown below:

$$FWHM_{175} = 8.97 \times 10^{-2} + 5.49 \times 10^{-4}(W.D.) \quad (2)$$

$$FWHM_{605} = 7.16 \times 10^{-2} + 7.66 \times 10^{-4}(W.D.) \quad (3)$$

where W.D. represents the work distance measured from the top of the vacuum chamber. With these two relationships, the work distances on the two machines can be adjusted to produce beams with the same FWHM values, thus allowing the work distance to be used as a variable to produce similar welds on different welders. A similar plot is made with the FWe2 values plotted as a function of work distance in Figure 10(b). The corresponding linear regressions for the two welders are shown below:

$$FWe2_{175} = 1.56 \times 10^{-1} + 8.68 \times 10^{-4}(W.D.) \quad (4)$$

$$FWe2_{605} = 1.11 \times 10^{-1} + 1.29 \times 10^{-3}(W.D.) \quad (5)$$

A comparison between the peak power density measurements of the beams produced by each welder at the machine sharp focus setting and the various work distances is shown in Figure 11. Overlaid on these experimental measurements are curves of the predicted peak power density, based on the FWHM relationships in Equations (2) and (3) and the following relationship for the peak power density (PPD) of the beam:

$$PPD(W / mm^2) = \frac{kV * mA}{2\pi \left(\frac{FWHM}{2.35} \right)^2} \quad (6)$$

where kV is the beam voltage and mA is the beam current. The relationship shown in Equation (4) is based on the assumption that each welder produces a Gaussian-shaped beam at each work distance. The factor of 2.35 in the above relationship originates from the relationship between the FWHM value for an ideal Gaussian beam and its standard deviation.[7]

Using these relationships, the work distance corresponding to a desired peak power density at the machine sharp focus can be predicted for each welder. The plot also shows that equivalent peak power density values at different work distances for two or more welders can also be

predicted. This plot also shows that there are differences in the performance of the two welders and that at a given work distance, the two welders produce sharply focused beams with different peak power densities. Overall, though, beams produced by different machines can be matched by changes in either the work distance or focus settings.

Since changes in work distance have such a pronounced impact on the beam parameters, a similar response is expected with the resulting weld dimensions. Figures 12(a-e) show micrographs of the weld pool cross sections corresponding to welds made under sharp focus conditions at five different work distances examined on S/N 175. As with the beam parameters, the changes in work distance have a significant impact on the size and shape of the resulting weld pool cross sections. In addition to changes in the measured weld dimensions, the general shapes of the weld cross sections change as well. For example, the welds made at the shorter work distances, as shown in Figures 12(a) and 12(b), exhibit a narrow keyhole region and a sharp point at the maximum depth. As the work distance is increased, the keyhole region widens, and the bottom of the weld becomes blunted. Similar behavior is displayed with the welds produced using S/N 605.

Summaries of the weld pool dimensions for S/N 175 and S/N 605 are listed in Tables 3 and 4, respectively. Comparisons between the depth, width, aspect ratio, and cross section area of the welds made at machine sharp focus settings on these two welders are also plotted in Figures 13(a) through 13(d) as a function of work distance. In each plot, the measured depths, widths, and cross sectional areas of the welds made on S/N 175 and S/N 605 are very similar over the range of work distances. It is worth noting, though, that the two welders display different trends in each of the measured weld dimensions across the range of work distances. This variation in trends may be an indication of other unaddressed factors which affect the properties of the beams produced by each welder.

Estimation of the Beam Crossover Location

The work distance has been defined up to this point as the distance from the top of the chamber to the surface of the work piece. This definition of the work distance provides a means for consistently placing the work piece at the same location in the chamber of each welder. However, this measurement is really only applicable on the welder on which it is made and can not be easily transferred to another welder, since differences in the construction of the upper

column of each welder are not taken into account. The effects of these variations in the construction of the two welders can be at least partly responsible for differences in the measured peak power density, beam distribution parameters, and resulting weld shapes and sizes at the sharp focus condition. A different means for defining the work distance across different welders is therefore required.

One such means involves the use of the distance between the electron focusing lens located in the upper column of the welder and the work piece. A schematic diagram of the upper column of a typical electron beam welder is shown in Figure 14. At the focus coils, the beam reaches its widest location. Physical measurements made in the upper column of each welder show that the focus lens in S/N 175 is located approximately 115 mm above the top of the vacuum chamber, while the focus lens in S/N 605 is located approximately 64 mm above the top of the chamber. These measurements represent only general locations for the focus coil and do not discriminate between the top, center, or bottom of the focus lens in the upper column.

Even though the location of the electron lens in the upper column is fixed, there are additional factors which can contribute to the observed variations in beam properties. For example, the upper column in each welder may be aligned differently or maintained under different vacuum levels. The performance of the electron focus lens can also vary due to differences in construction or degradation over time. Such unique internal characteristics are difficult to quantify when comparing different welders and may affect the beam properties in unknown ways even under the same experimental conditions. Since the location of these coils and their performance varies between welders, they are not suitable for defining a standard work distance to be used between welders. Therefore, it becomes necessary to develop a means for taking into account other more difficult to quantify differences in machine performance.

On the other hand, a beam crossover point, where the beam diameter is effectively zero, is present in the general location of the anode. The crossover point depends on the gun design and can be correlated with the location of the anode. However, the electron guns used on the two systems are different, making a physical measurement of the anode inapplicable. It is also known that the locations of the anodes in the upper columns are mounted at different distances from the cathode in the electron gun.[11] These differences in the construction of the upper column obviously contribute to differences in the performance of the two welders. However, some means for quantifying these changes needs to be devised.

The theoretical beam crossover location can be estimated, though, using the results obtained with the EMFC on sharply focused beams at different work distances. Based on these data sets, the beam crossover point corresponds to the work distance where the electron gun would theoretically produce a sharply focused beam with a FWHM or FWe2 of zero. In Figures 10(a) and 10(b), the linear regressions of the measured beam distribution parameters are extended to FWHM and FWe2 values of zero. These intercept values correspond to the beam crossover location, and the two distribution parameters produce slightly different results for both machines. Based on these two sets of measurements, the beam crossover locations are located at approximately 170 mm above the top of the chamber for S/N 175 and 90 mm above the top of the chamber for S/N 605. Unlike physical measurements of the focus lens location, the estimation of this crossover point takes into account the performance of the welder and gives some meaning to difficult-to-define variables.

Summary and Conclusions

In this study, the performance characteristics of two welders in use at LLNL (S/N 175 and S/N 605) have been characterized using an advanced diagnostic tool for measuring the properties of electron beams. With this tool, the effects of changes in the focus setting on the peak power density and beam distribution parameters (FWHM and FWe2 values) for 1 kW beams have been determined. Differences are observed in the beam characteristics of each machine, even though the same machine settings are maintained in each system. In particular, differences in the size and shape of beams produced at the respective machine sharp focus settings are evident. The respective peak power density values vary by more than 20%, while the beam distribution parameters vary by approximately 12% at a work distance of 229 mm. The two sharply focused beams also display obvious differences in the power density distribution across the beam diameter and produce different sized welds.

The relationship between these well-characterized 1 kW electron beams and their resulting weld pool dimensions have been examined on 304L stainless steel samples. However, the presence of spiking in the weld produced by S/N 605 complicates any direct comparison of the two welds. When taking into account the spiking, the weld produced by S/N 175 at the machine sharp focus setting is approximately 17% deeper, which corresponds with its higher peak power density, which is 22% higher. Ignoring the spiking results in the weld produced by S/N 605

having a 7% higher depth. Differences in beam orientation and power density distribution are also observed when comparing the two beams, making it clear. Therefore, it is clear that knowledge of the power density distribution in the beam and beam shape and orientation is required to produce welds with similar dimensions on different machines.

The effects of work distance on the beam parameters have also been investigated over a range of work distances between 127 mm and 508 mm. These work distances are measured from the top of the welding chamber to the top of the work piece and have a dramatic influence on the beam properties. In particular, the peak power density values measured at the longer work distances are much lower than those measured at the shorter work distances, while the beam distribution parameters become much wider at longer work distances. This variation in work distance resulted in an approximate 33% decrease in the weld depth when using the sharpest focused beam at each work distance on S/N 175. Similar changes in the measured weld depths are also observed with changes in work distance on S/N 605.

Additional differences are also observed when comparing the performance of the two welders, indicating that other factors are contributing to machine performance. In order to take into account these differences in machine performance, the theoretical location of beam crossover in the upper column of each machine has been determined. This value is based on measurements of the FWHM beam distribution parameter at the sharp focus setting over a range of work distances in each welder and its extrapolation to a value of zero. Each machine displays a unique beam crossover location in the machine upper column, with values of 163 mm and 83 mm being determined for S/N 175 and S/N 605, respectively.

Acknowledgments

The LLNL portion of this work was performed under the auspices of the U.S. Department of Energy by University of California, Lawrence Livermore National Laboratory under Contract W-7405-Eng-48. The authors would also like to acknowledge the contributions of Mr. Alan Teruya (LLNL) for his substantial software development support and Mr. Robert Vallier (LLNL) and Mr. Jackson Go (LLNL) for performing the metallography on the weld samples.

References

1. Recommended Practices for Electron Beam Welding, 2004, AWS C7.1M/C7.1:2004, Miami,

FL, American Welding Society.

2. G. R. LaFlamme and D. E. Powers: *Welding Journal*, 1991, **70**(10): pp. 33-40.
3. U. Diltthey and J. Weiser: *Schw. and Schn.*, 1995, **47**(7): pp. 558-564.
4. U. Diltthey and J. Weiser: *Schw. and Schn.*, 1995, **47**(5): pp. 339-345.
5. J. W. Elmer and A. T. Teruya, "An Enhanced Faraday Cup for the Rapid Determination of the Power Density Distribution in Electron Beams," *Welding Journal*, **80**(12), 288s-295s, 2001.
6. J.W. Elmer and A.T. Teruya, "Fast Method for Measuring Power Density Distribution of Non-Circular and Irregular Electron Beams," *Science and Technology of Welding and Joining*, **3**(2), 51-58, 1998.
7. J.W. Elmer, A.T. Teruya, and D.W. O'Brien, "Tomographic Imaging of Noncircular and Irregular Electron Beam Current Density Distributions," *Welding Journal*, **72**(11), 493s-505s, 1993.
8. A. Teruya, J. Elmer, and D. O'Brien, "A System for the Tomographic Determination of the Power Distribution in Electron Beams," in The Laser and Electron Beam in Welding, Cutting, and Surface Treatment: State-of-the-Art 1991, Bakish Materials Corp., Englewood, NJ, 1991, pp. 125-140.
9. J.W. Elmer, A.T. Teruya, and T.A. Palmer, "User's Guide: An Enhanced Modified Faraday Cup for the Profiling of the Power Density Distribution in Electron Beams", Lawrence Livermore National Laboratory Document UCRL-MA-148830, 2002.
10. R.E. Armstrong, "Control of Spiking in Partial Penetration Electron Beam Welds", *Weld. J.*, 1970, **49**(8), 382s-388s.
11. C.W. Weidner and L.E. Shuler, "Effect of Process Variables on Partial Penetration Electron Beam Welding", *Weld. J.*, 1973, **52**(3), 114s-119s.
12. G.L. Mara, E.R. Funk, R.C. McMaster, and P.E. Pence, "Penetration Mechanisms of Electron Beam Welding and the Spiking Phenomenon", *Weld. J.*, 1974, **53**(6), 246s-251s.
13. C.M. Weber, E.R. Funk, and R.C. McMaster, "Penetration Mechanism of Partial Penetration Electron Beam Welding", *Weld. J.*, 1972, **51**(2), 90s-94s.
14. H. Tong and W.H. Giedt, "A Dynamic Interpretation of Electron Beam Welding", *Weld. J.*, 1970, **49**(6), 259s-266s.
15. T.A. Palmer, J.W. Elmer, K.D. Nicklas, T. Mustaleski, and P. Burgardt, unpublished research, 2004.

List of Tables

Table 1. Chemical composition of 304L stainless steel samples used in the round robin welding study. All values are in wt.%.

Table 2. Summary of electron beam characteristics measured in each welder during the round robin tests for welds made at 100 kV, 10 mA machine settings and a work distance of 229 mm. All welds are made at a travel speed of 17 mm/sec.

Table 3. Summary of beam parameters made at the machine sharp focus setting measured at each work distance on S/N 175 for a 100 kV, 10 mA beam. All welds are made at a travel speed of 17 mm/sec.

Table 4. Summary of beam parameters made at the machine sharp focus setting measured at each work distance on S/N 605 for a 100 kV, 10 mA beam. All welds are made at a travel speed of 17 mm/sec.

List of Figures

Figure 1(a&b). (a) Photograph of the Enhanced Modified Faraday Cup and (b) a schematic cross sectional illustration of the EMFC diagnostic with the following components identified: a. an internal slit disk made of copper, b. an internal beam trap, c. graphite beam interceptors, d. a clamp for the tungsten slit disk, and e. an integral BNC connector.

Figure 2(a-d). Basic overview of operation of the EMFC system beginning with (a) a typical profile acquire through one of the slits, (b) a computed sinogram compiling the profiles seen by all 17 slits, (c) a 3D tomographic reconstruction of the power density distribution of the beam, and (d) a slice through the center of the reconstructed beam with the peak power density, FWHM, and FWe2 measurements indicated.

Figure 3(a&b). (a) Peak power density plotted as a function of the focus coil current for the defocus run made on S/N 175, showing the operator determined sharp focus. (b) The same data plotted as a function of the relative machine focus setting, where the zero value for the relative machine focus setting corresponds to the focus setting at which the maximum peak power density is measured.

Figure 4(a&b). Plots comparing the reconstructed beams produced at the machine sharp focus settings for 100 kV, 10 mA beams at a work distance of 229 mm on (a) S/N 175 and (b) S/N 605.

Figure 5(a-c). Plots comparing the measured (a) peak power density, (b) FWHM values, and (c) FWe² values with changes in the focus setting on each welder for 100 kV, 10 mA beams at a work distance of 229 mm.

Figure 6(a&b). Weld cross sections produced in 304L stainless steel samples at the machine sharp focus setting for 100 kV, 10 mA beams at a work distance of 229 mm and a travel speed of 17 mm/sec on the (a) S/N 175 (PPD=20.0 kW/mm²) and (b) S/N 605 (PPD = 15.7 kW/mm²).

Figure 7(a-c). Plots comparing the measured (a) peak power density, (b) FWHM values, and (c) FWe2 values with changes in the focus setting for 100 kV, 10 mA beams at several different work distances on the S/N 175.

Figure 8(a-c). Plots comparing the measured (a) peak power density, (b) FWHM values, and (c) FWe2 values with changes in the focus setting for 100 kV, 10 mA beams at several different work distances on S/N 605.

Figure 9. Plot showing the relationship between the work distance and the FWHM and FWe2 values measured on S/N 175 at the machine sharp focus setting for 100 kV, 10 mA beams.

Figure 10. Comparisons between the FWHM values measured at sharp focus settings for both welders as a function of work distance for 100 kV, 10 mA beams.

Figure 11. Comparison between peak power density values measured at sharp focus settings for the three welders as a function of work distance for 100 kV, 10 mA beams. The theoretical peak power density for each welder is also plotted as a function of the work distance.

Figure 12(a-e). Micrographs showing cross sections from welds made at machine sharp focus settings on S/N 175 with 100 kV, 10 mA beams at a travel speed of 17 mm/sec and work distances of (a) 127 mm, (b) 229 mm, (c) 305 mm, (d) 381 mm, and (e) 457 mm.

Figure 13(a-d). Comparison between measurements of the cross section (a) depth, (b) width, (c) aspect ratio, and (d) area for welds made on both welders (S/N 175 and S/N 605) with 100 kV, 10 mA beams at a travel speed of 17 mm/sec.

Table 1. Characteristics of electron beam welders used in this study.

	Welder #1	Welder #2
<i>Manufacturer</i>	Hamilton Standard	Hamilton Standard
<i>Serial number</i>	175	605
<i>Voltage (kV)</i>	150	150
<i>Current (mA)</i>	50	50
<i>Filament Type</i>	Ribbon*	Ribbon*
<i>Electron Gun Type</i>	R167-R	CL-R167-R
<i>Year of Manufacture</i>	1965	1975

* Ribbon filament upgrade made to machine circa 1990.

Table 2. Summary of electron beam characteristics measured in each welder during the round robin tests for welds made at 100 kV, 10 mA machine settings and a work distance of 229 mm. All welds are made at a travel speed of 17 mm/sec.

	S/N 175	S/N 605
Focus Coil Current (mA) at the machine sharp focus setting	446	672
Peak Power Density (kW/mm ²)	20.0	15.7
FWHM (mm)	0.210	0.237
FWe2 (mm)	0.346	0.395
Weld Depth (mm)	3.97	4.26
Weld Width (mm)	1.49	1.43
Aspect Ratio	2.67	2.98
Cross Sectional Area (mm ²)	2.63	2.69

Table 3. Summary of beam parameters made at the machine sharp focus setting measured at each work distance on S/N 175 for a 100 kV, 10 mA beam. All welds are made at a travel speed of 17 mm/sec.

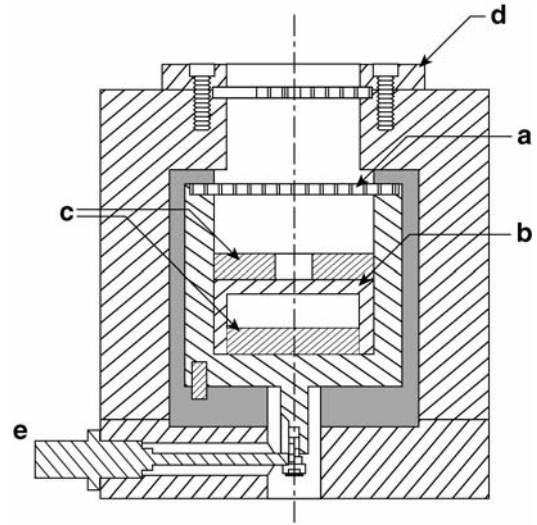
	Work Distance (H.S. S/N 175)					
	<i>127 mm</i>	<i>184 mm</i>	<i>229 mm</i>	<i>305 mm</i>	<i>381 mm</i>	<i>457 mm</i>
Peak Power Density (kW/mm²)	34.9	21.6	20.0	14.1	10.2	7.79
FWHM (mm)	0.155	0.204	0.210	0.251	0.298	0.344
FWe2 (mm)	0.262	0.332	0.346	0.413	0.486	0.557
Weld Depth (mm)	4.46	4.21	3.97	3.69	3.39	2.96
Weld Width (mm)	1.27	1.29	1.48	1.48	1.55	1.71
Aspect Ratio	3.52	3.27	2.65	2.49	2.19	1.73
Cross Sectional Area (mm²)	2.40	2.55	2.63	2.58	2.56	2.62

Table 4. Summary of beam parameters made at the machine sharp focus setting measured at each work distance on S/N 605 for a 100 kV, 10 mA beam. All welds are made at a travel speed of 17 mm/sec.

	Work Distance (S/N 605)					
	<i>178 mm</i>	<i>229 mm</i>	<i>305 mm</i>	<i>381 mm</i>	<i>457 mm</i>	<i>508 mm</i>
Peak Power Density (kW/mm²)	19.3	15.7	10.8	6.19	4.34	4.80
FWHM (mm)	0.210	0.237	0.290	0.390	0.455	0.423
FWe2 (mm)	0.353	0.395	0.473	0.635	0.736	0.732
Weld Depth (mm)	4.38	4.26/3.42	3.55	3.30	2.91	2.79
Weld Width (mm)	1.41	1.43	1.60	1.63	1.85	1.85
Aspect Ratio	3.10	2.98/2.39	2.23	2.03	1.57	1.51
Cross Sectional Area (mm²)	2.62	2.69	2.61	2.57	2.49	2.49



(a)



(b)

Figure 1(a&b). (a) Photograph of the Enhanced Modified Faraday Cup and (b) a schematic cross sectional illustration of the EMFC diagnostic with the following components identified: a. an internal slit disk made of copper, b. an internal beam trap, c.graphite beam interceptors, d. a clamp for the tungsten slit disk, and e. an integral BNC connector.

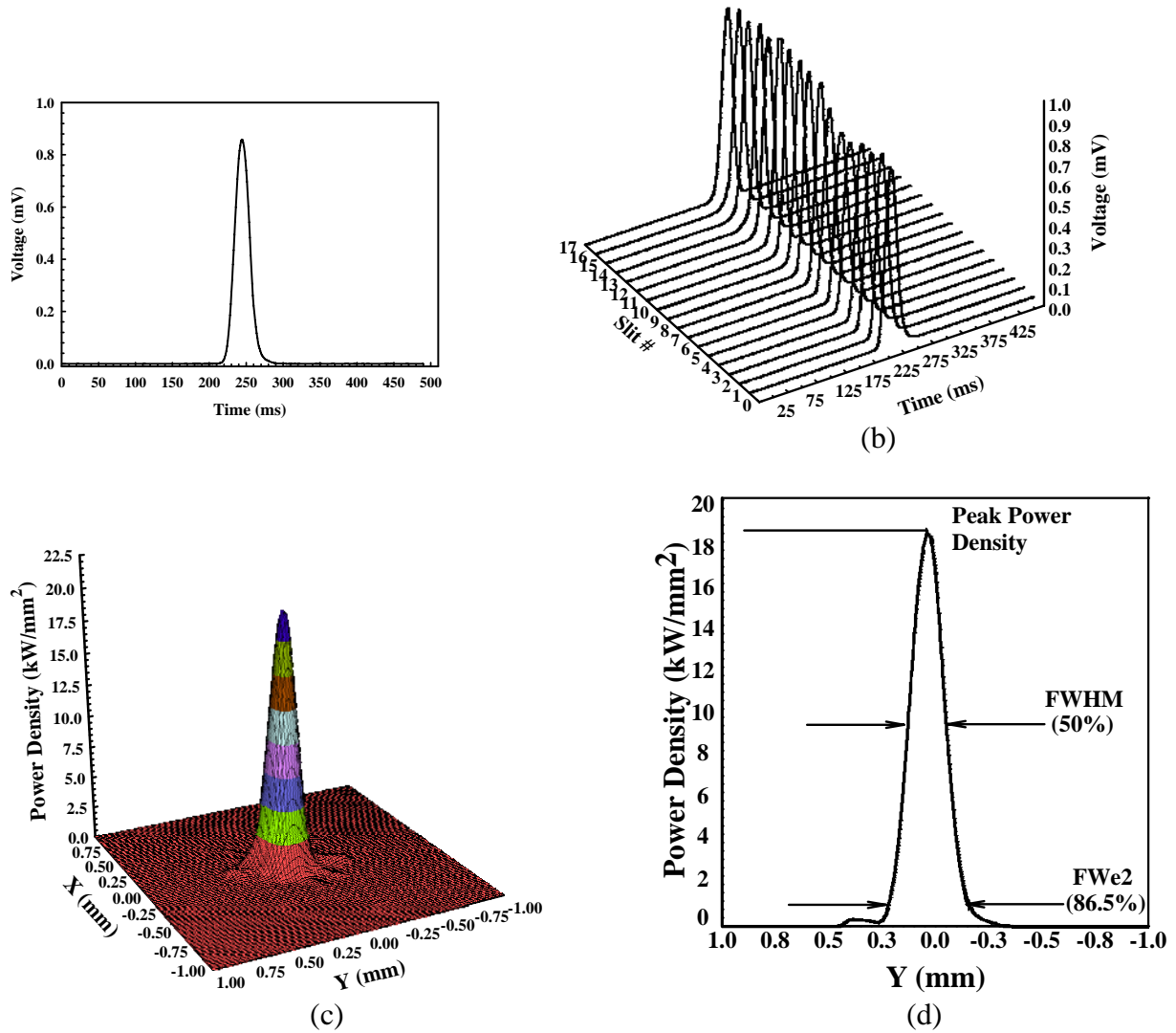


Figure 2(a-d). Basic overview of operation of the EMFC system beginning with (a) a typical profile acquire through one of the slits, (b) a computed sinogram compiling the profiles seen by all 17 slits, (c) a 3D tomographic reconstruction of the power density distribution of the beam, and (d) a slice through the center of the reconstructed beam with the peak power density, FWHM, and FWe2 measurements indicated.

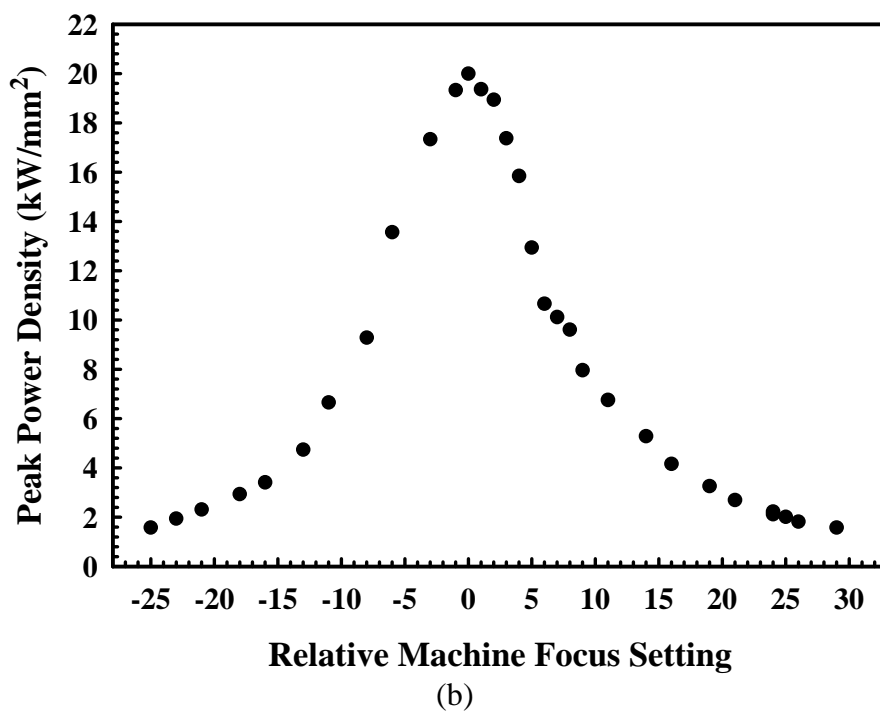
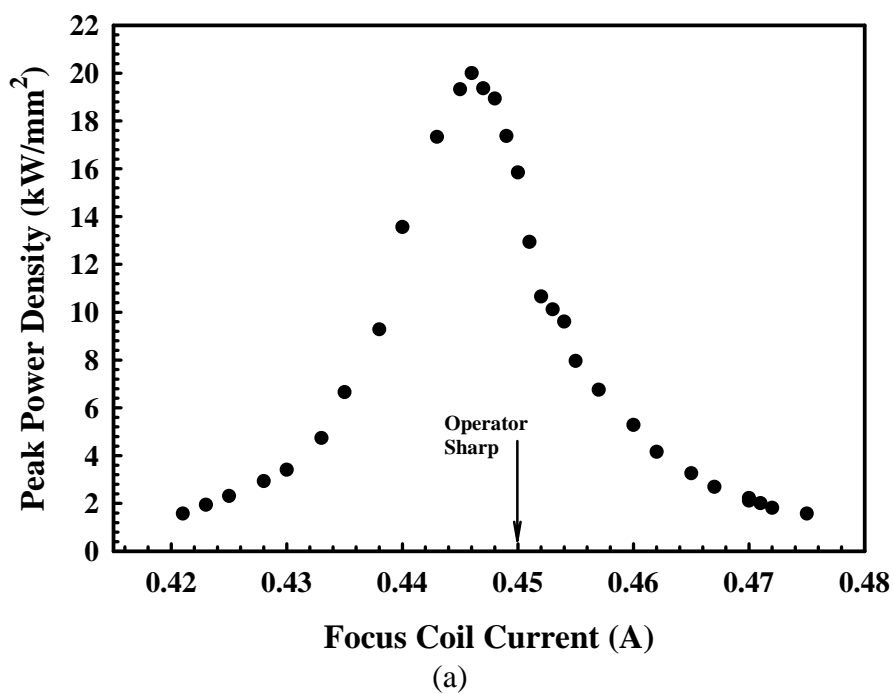


Figure 3(a&b). (a) Peak power density plotted as a function of the focus coil current for the defocus run made on S/N 175, showing the operator determined sharp focus. (b) The same data plotted as a function of the relative machine focus setting, where the zero value for the relative machine focus setting corresponds to the focus setting at which the maximum peak power density is measured.

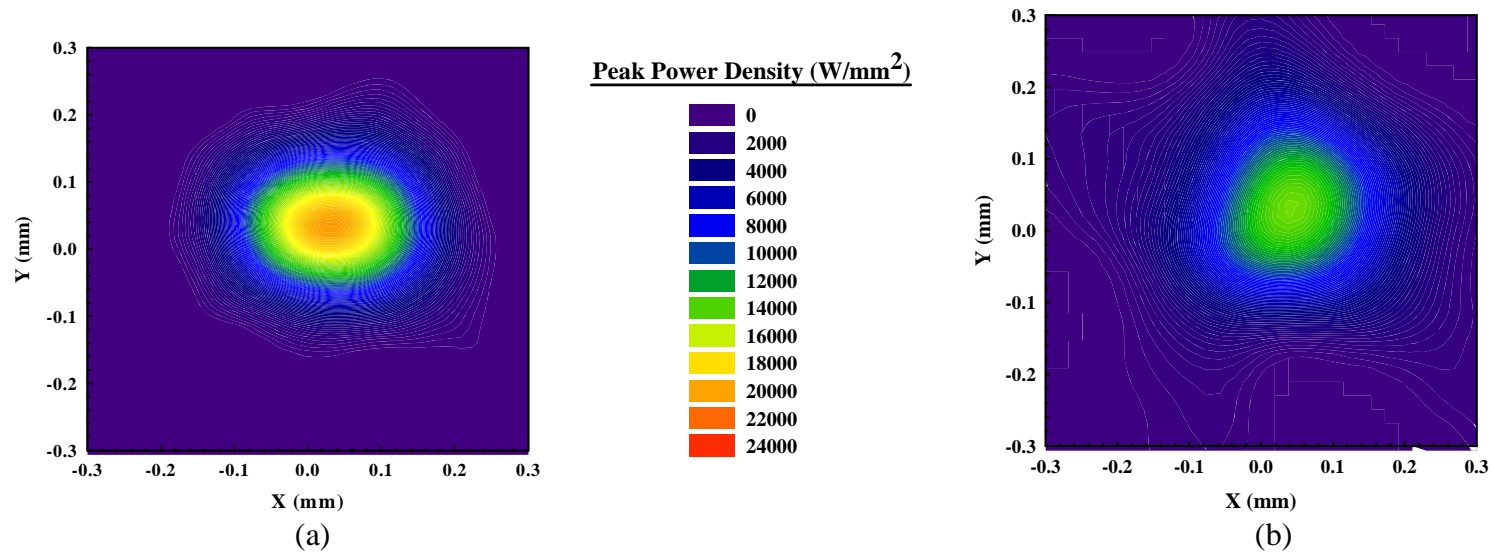


Figure 4(a&b). Plots comparing the reconstructed beams produced at the machine sharp focus settings for 100 kV, 10 mA beams at a work distance of 229 mm on (a) S/N 175 and (b) S/N 605.

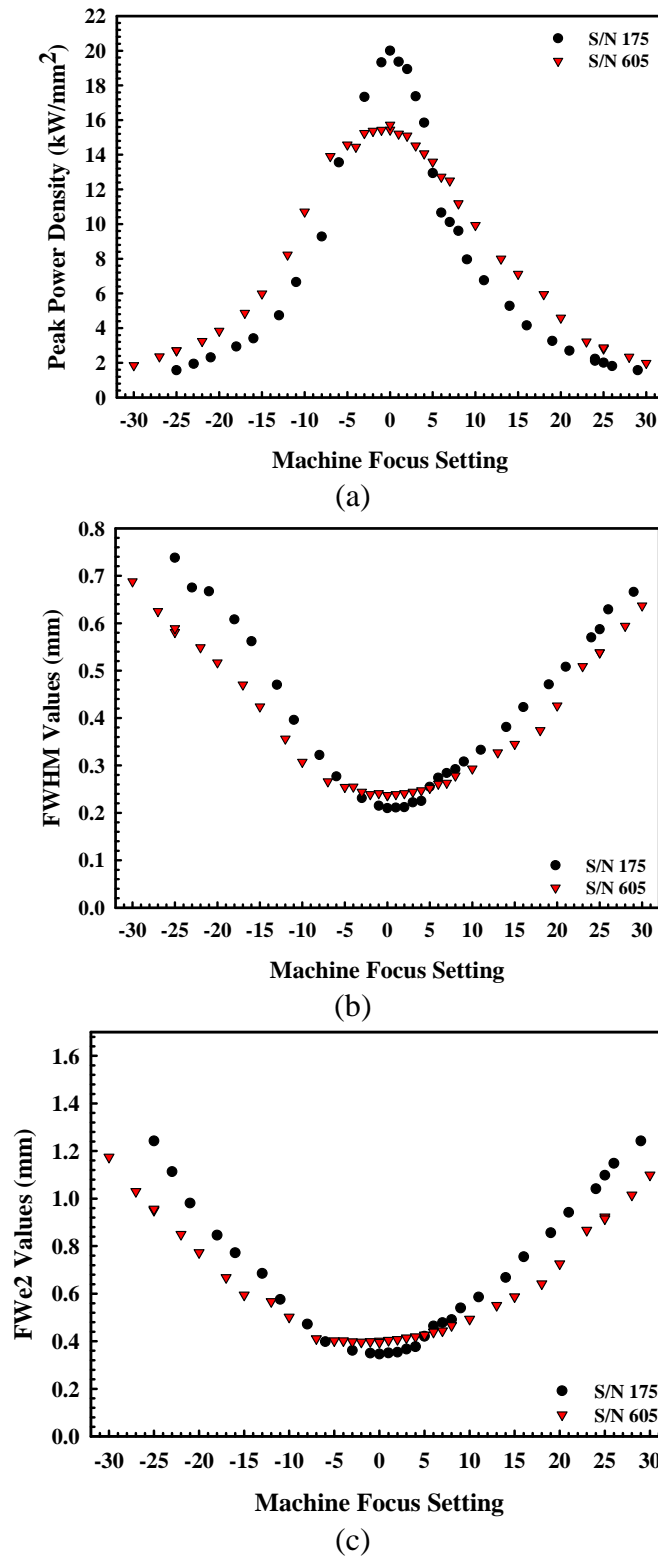
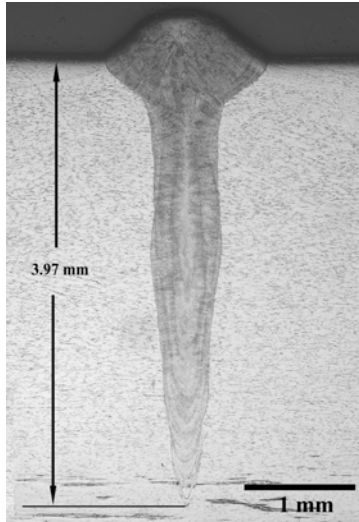
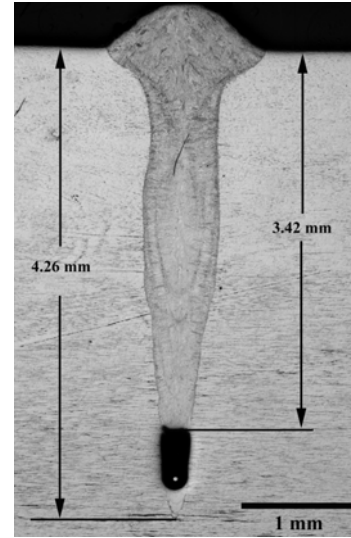


Figure 5(a-c). Plots comparing the measured (a) peak power density, (b) FWHM values, and (c) FWe² values with changes in the focus setting on each welder for 100 kV, 10 mA beams at a work distance of 229 mm.

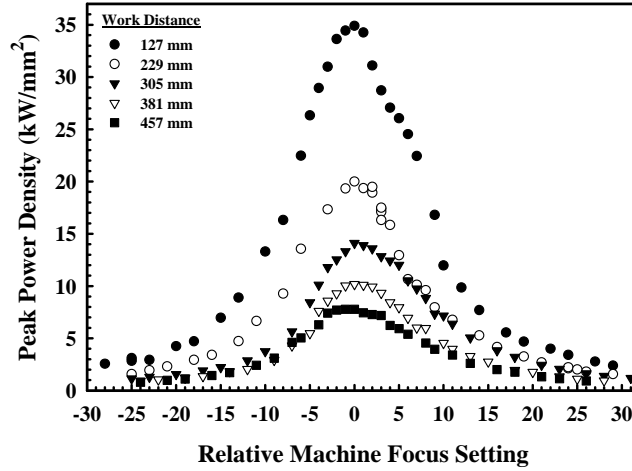


(a)

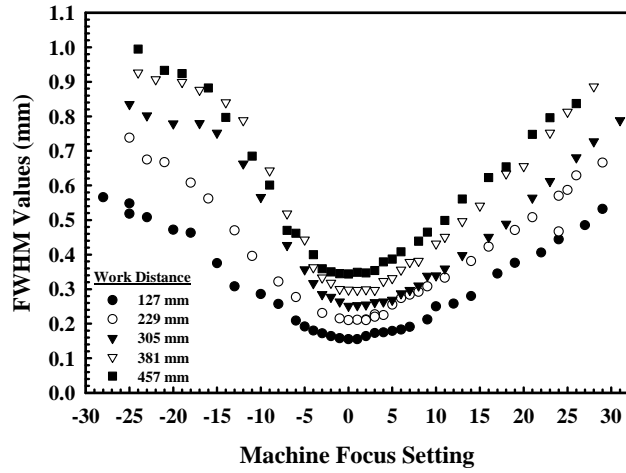


(b)

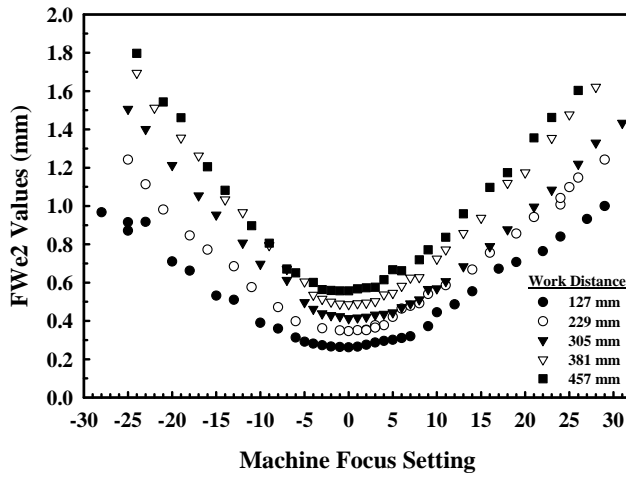
Figure 6(a&b). Weld cross sections produced in 304L stainless steel samples at the machine sharp focus setting for 100 kV, 10 mA beams at a work distance of 229 mm and a travel speed of 17 mm/sec on the (a) S/N 175 (PPD=20.0 kW/mm²) and (b) S/N 605 (PPD = 15.7 kW/mm²).



(a)



(b)



(c)

Figure 7(a-c). Plots comparing the measured (a) peak power density, (b) FWHM values, and (c) FWe2 values with changes in the focus setting for 100 kV, 10 mA beams at several different work distances on S/N 175.

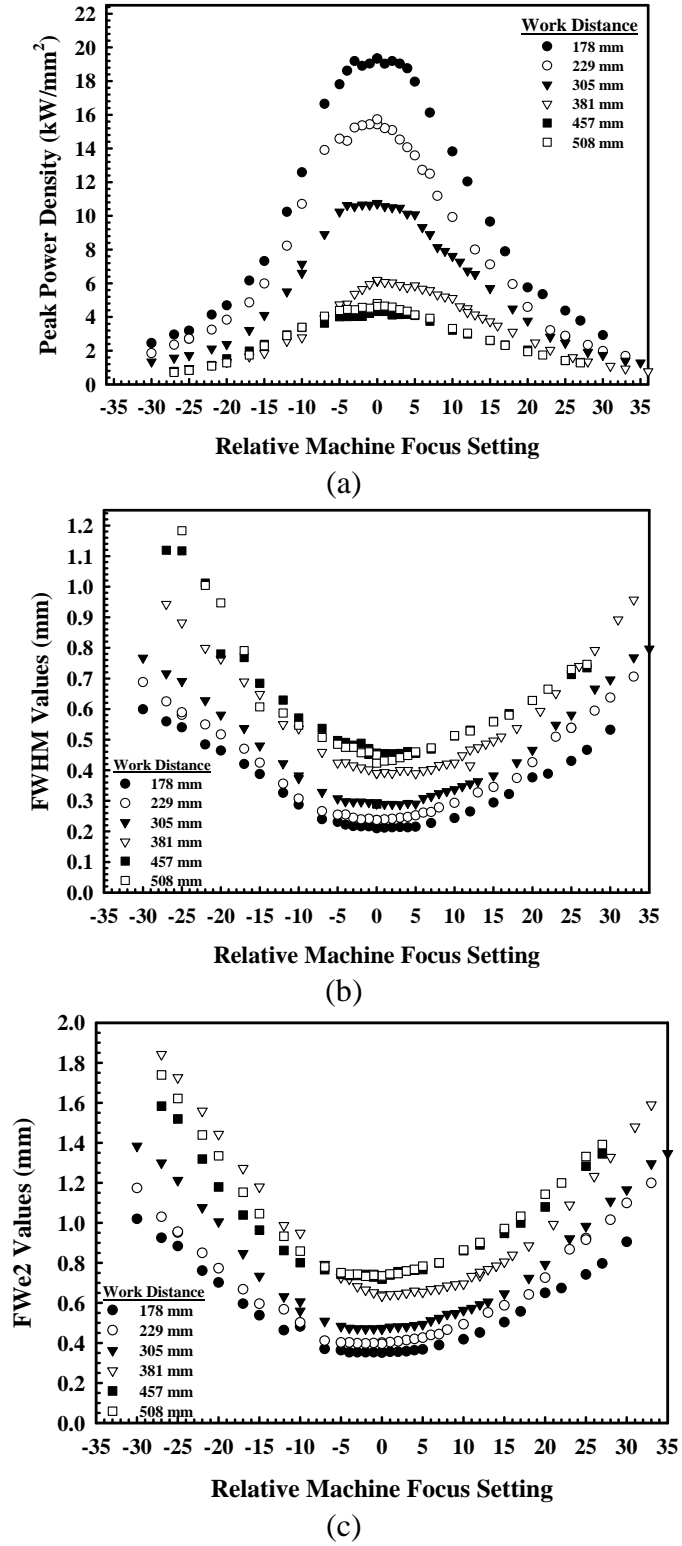


Figure 8(a-c). Plots comparing the measured (a) peak power density, (b) FWHM values, and (c) FWe2 values with changes in the focus setting for 100 kV, 10 mA beams at several different work distances on S/N 605.

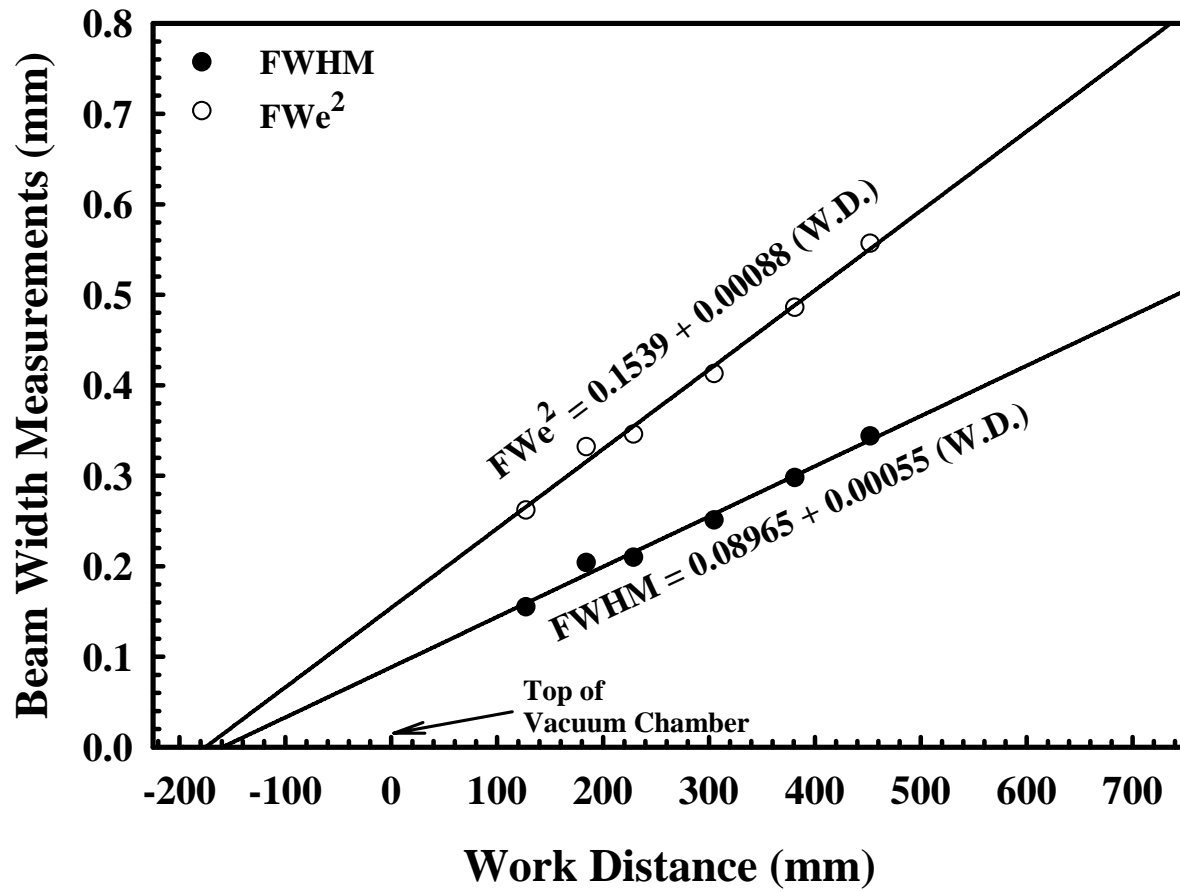
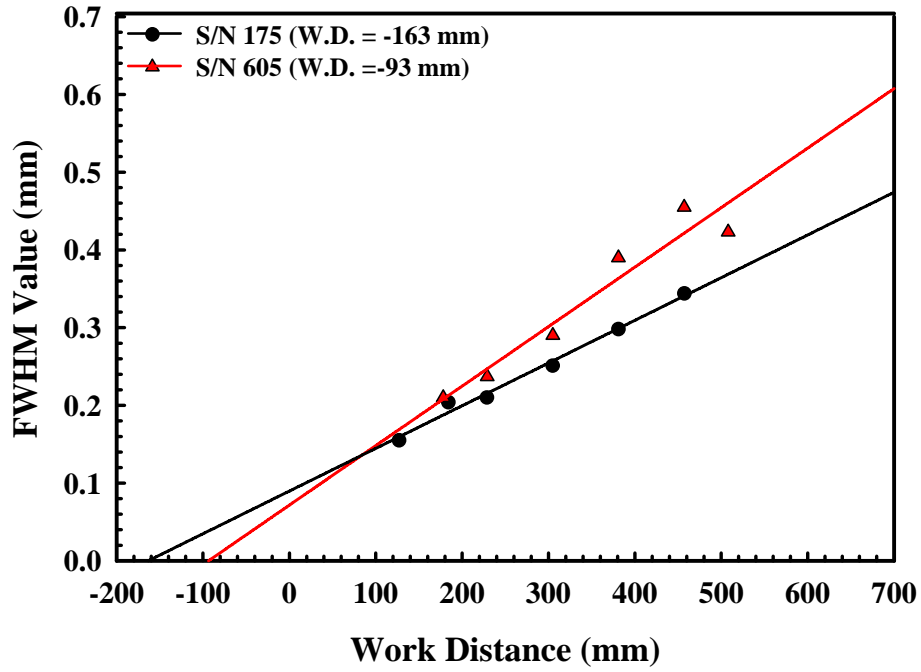
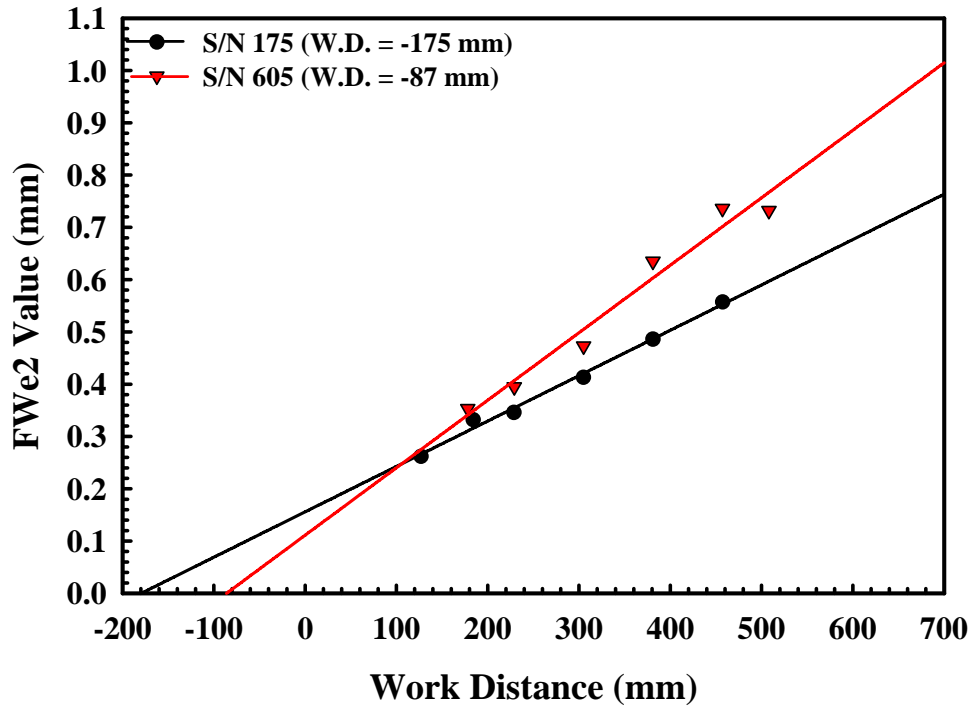


Figure 9. Plot showing the relationship between the work distance and the FWHM and FWe² values measured on S/N 175 at the machine sharp focus setting for 100 kV, 10 mA beams.



(a)



(b)

Figure 10(a&b). Comparisons between the (a) FWHM values and (b) FWe2 values measured at sharp focus settings for both welders as a function of work distance for 100 kV, 10 mA beams.

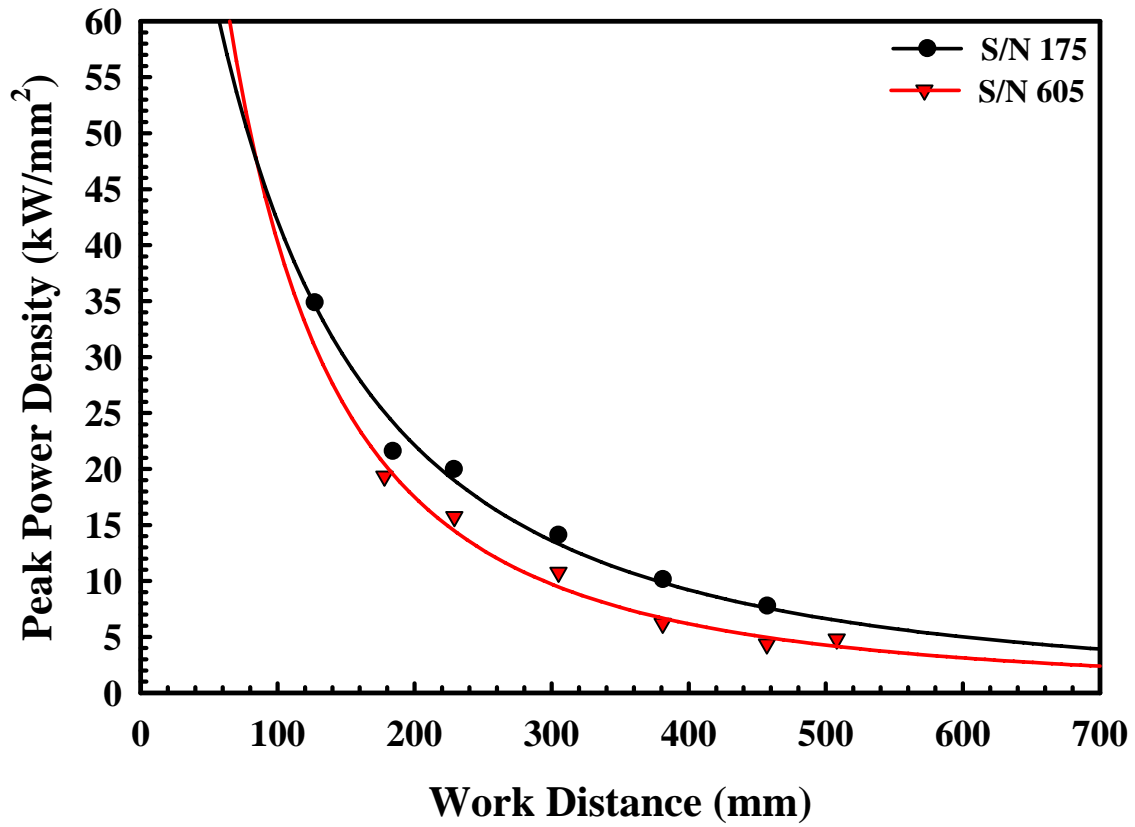


Figure 11. Comparison between peak power density values measured at sharp focus settings for the three welders as a function of work distance for 100 kV, 10 mA beams. The theoretical peak power density for each welder is also plotted as a function of the work distance.

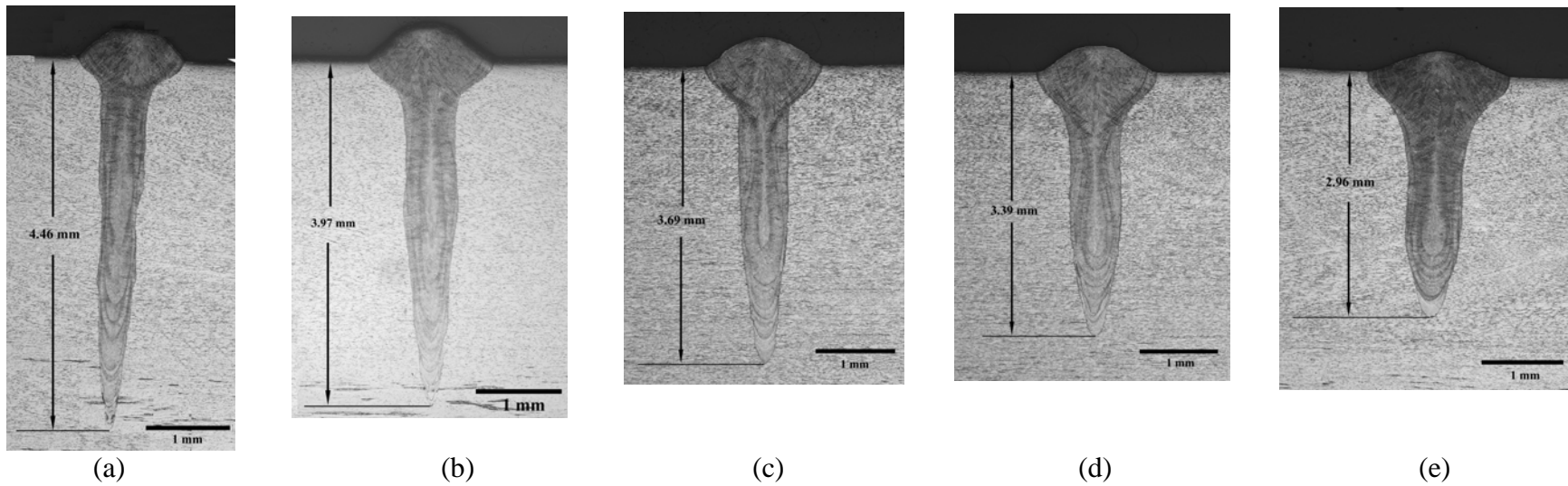
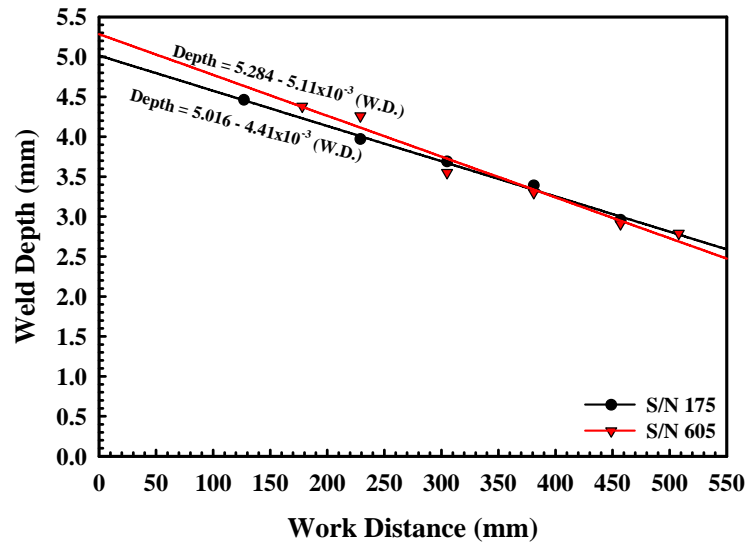
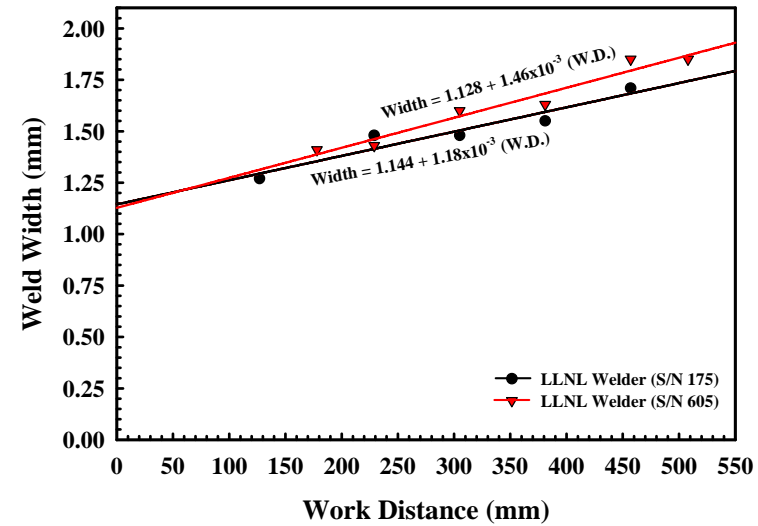


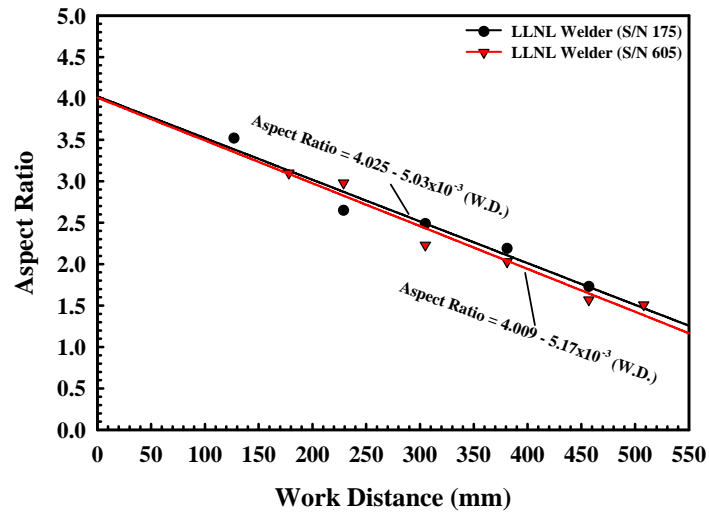
Figure 12(a-e). Micrographs showing cross sections from welds made at machine sharp focus settings on EB welder S/N 175 with 100 kV, 10 mA beams at a travel speed of 17 mm/sec and work distances of (a) 127 mm, (b) 229 mm, (c) 305 mm, (d) 381 mm, and (e) 457 mm.



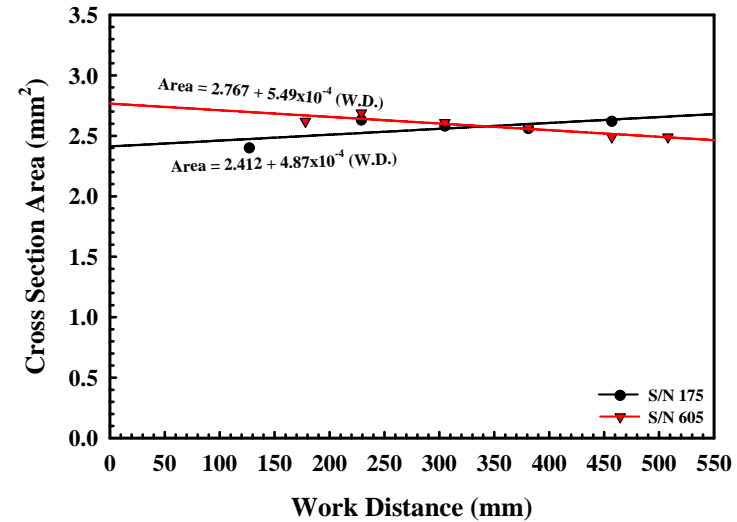
(a)



(b)



(c)



(d)

Figure 13(a-d). Comparison between measurements of the cross section (a) depth, (b) width, (c) aspect ratio, and (d) area for welds made on both welders (S/N 175 and S/N 605) with 100 kV, 10 mA beams at a travel speed of 17 mm/sec.